Abrupt shoaling of the nutricline in response to massive freshwater flooding at the onset of the last interglacial sapropel event

Michaël Grelaud,[1] Gianluca Marino,[1] Patrizia Ziveri,[1,2] and Eelco J. Rohling[3]

Received 23 January 2012; revised 25 May 2012; accepted 22 June 2012; published 30 July 2012.

[1] A detailed assessment of the respective roles of production, export, and subsequent preservation of organic carbon (C_{org}) in the eastern Mediterranean (EMED) sediments during the formation of sapropels remains elusive. Here we present new micropaleontological results for both surface samples taken at several locations in the EMED and last interglacial sapropel S5 from core LC21 in the southeastern Aegean Sea. A strong exponential anticorrelation between relative abundances of the lower photic zone coccolithophore *Florisphaera profunda* in the surface sediments and modern concentrations of chlorophyll a (Chl-a) at the sea surface suggests that *F. profunda* percentages can be used to track past productivity changes in the EMED. Prior to S5 deposition, an abrupt and large increase of *F. profunda* percentages in LC21 coincided (within the multidecadal resolution of the records) with the marked freshening of EMED surface waters. This suggests a strong coupling between freshwater-bound surface to intermediate water (density) stratification and enhanced upward advection of nutrients to the base of the photic zone, fuelling a productive deep chlorophyll maximum (DCM) underneath a nutrient-starved surface layer. Our findings imply that (at least) at the onset of sapropel formation physical and biogeochemical processes likely operated in tandem, enabling high C_{org} accumulation at the seafloor.

Citation: Grelaud, M., G. Marino, P. Ziveri, and E. J. Rohling (2012), Abrupt shoaling of the nutricline in response to massive freshwater flooding at the onset of the last interglacial sapropel event, *Paleoceanography*, *27*, PA3208, doi:10.1029/2012PA002288.

1. Introduction

[2] The Mediterranean Sea is a semi-enclosed marginal sea of the Atlantic Ocean with a generally well-ventilated water column owing to multiple sites of intermediate to deep convection and a vigorous basin-wide thermohaline circulation [*Zavatarielli and Mellor*, 1995; *Pinardi and Masetti*, 2000]. The latter is largely driven by excess evaporation and related water mass transformation within the eastern Mediterranean (EMED) (i.e., east of the Strait of Sicily) and is thus very sensitive to changes in the freshwater budget of that sector of the basin [e.g., *Rohling and Bryden*, 1992]. EMED sapropels are organic-rich layers that reflect curtailed bottom water ventilation [*Rohling*, 1994; *Cramp and O'Sullivan*, 1999; *Negri et al.*, 2009] during periods of orbital precession minima [*Revel et al.*, 2010; *Ziegler et al.*, 2010], in response to enhanced monsoon-fuelled river discharge along the North African margin [e.g., *Rohling et al.*, 2002, 2004; *Osborne et al.*, 2008]. The freshwater-bound weakening of the EMED thermohaline circulation inhibited oxygen supply to the deep sea, thereby promoting organic carbon (C_{org}) preservation at depth [e.g., *Rossignol-Strick et al.*, 1982; *Rohling*, 1994; *De Lange et al.*, 2008]. Other studies suggest that enhanced primary productivity in the upper water column during periods of sapropel deposition increased the downward export of C_{org}, in turn, enabling deep-water anoxia [e.g., *De Lange and ten Haven*, 1983; *Calvert et al.*, 1992].

[3] Although the debate is often presented in polarized terms of "anoxia" versus "productivity," the actual evidence instead alludes to a combination of these influences, which can be viewed as components of a single underlying hydrographic response to freshwater forcing [*Rohling and Gieskes*, 1989; *Rohling*, 1994]. For example, microfossil assemblages [*Rohling and Gieskes*, 1989; *Castradori*, 1993; *Kemp et al.*, 1999] and geochemical data [*Sachs and Repeta*, 1999] in certain sapropels point to the occurrence of a productive deep chlorophyll maximum (DCM) positioned underneath a nutrient-impoverished mixed layer. The shoaling of the isopycnals in response to surface freshening would then explain the upward advection of nutrients [*Rohling and Gieskes*, 1989] that were either "concentrated" in the basin due to a sluggish thermohaline circulation [*Sarmiento et al.*, 1988], accumulated over a considerable period of time prior to the deep-water ventilation changes [*Casford et al.*, 2002], or

[1]Institut de Ciència i Tecnologia Ambientals, Universitat Autònoma de Barcelona, Bellaterra, Spain.
[2]Earth and Climate Cluster, Department of Earth Sciences, FALW, Vrije Universiteit Amsterdam, Amsterdam, Netherlands.
[3]School of Ocean and Earth Science, National Oceanography Centre, University of Southampton, Southampton, UK.

Corresponding author: M. Grelaud, Institut de Ciència i Tecnologia Ambientals, Universitat Autònoma de Barcelona, ES-08193 Bellaterra, Spain. (michael.grelaud@uab.cat)

0883-8305/12/2012PA002288

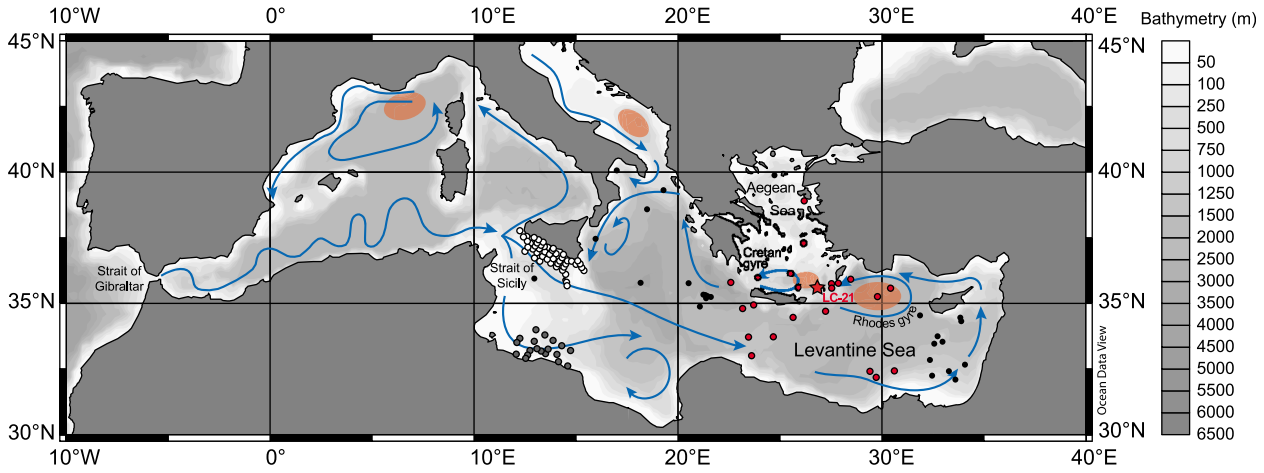

Figure 1. Map of the Mediterranean Sea showing the main patterns of surface water circulation [*Pinardi and Masetti*, 2000], blue arrows; and location of deep water formation sites, red areas. The red star indicates the location of core LC21. Red, white and gray circles show the location of the surface sediment samples that were used for the distribution of *F. profunda* in Figure 2a and the reconstructions presented in Figure 2c. The black circles depict the location of the surface sediment samples only used for the distribution of *F. profunda* in Figure 2a. A complete list of these samples is given in Table S1 in the auxiliary material.

"regenerated" under oxygen-depleted conditions [*Slomp et al.*, 2002]. This picture is contrasted with the present-day EMED, for which sediments are strongly depleted in C_{org} due to ultra-oligotrophic and phosphorus-starved surface waters [*Krom et al.*, 1991; *Turley et al.*, 2000; *D'Ortenzio and Ribera d'Alcalà*, 2009]. The latter is a reflection of a net westward export of dissolved nutrients across the Strait of Sicily that is coupled with the efficient anti-estuarine circulation (and vigorous deep ventilation) in the Mediterranean Sea [*Ignatiades et al.*, 2009; *Siokou-Frangou et al.*, 2010].

[4] Clearly there is a tight interplay between physical and biogeochemical processes in the EMED, suggesting that vertical fluxes and utilization of nutrients in the upper water column may respond dramatically to perturbations of the basin's thermohaline circulation (for example by freshwater forcing). Deciphering timing and magnitude of these responses is critical for unraveling the mechanisms that control sapropel formation. Recent high-resolution studies have detailed the picture of the physical processes associated with the deposition of sapropels [*Casford et al.*, 2002, 2003; *Rohling et al.*, 2002, 2004, 2006; *Marino et al.*, 2007, 2009], but there remains a need for similarly resolved reconstructions of the contemporaneous productivity patterns.

[5] Here we focus on the last interglacial sapropel S5, a strongly developed anoxic event in the EMED [*Kemp et al.*, 1999; *Rohling et al.*, 2002, 2004, 2006; *Marino et al.*, 2007; *Osborne et al.*, 2008, 2010]. Sapropel S5, as opposed to the more recent S1 [*Mercone et al.*, 2001; *Casford et al.*, 2002, 2003], is intensively developed in terms of (i) freshwater forcing [*Rohling et al.*, 2002], (ii) severity of the hydrographic responses throughout the basin [*Rohling et al.*, 2006; *Marino et al.*, 2007], and (iii) accumulation of organic carbon (C_{org}) at the seafloor [*Kemp et al.*, 1999; *Struck et al.*, 2001; *Rohling et al.*, 2006; *Marino et al.*, 2007]. The high signal-to-noise ratios in S5 make this anoxic event ideally suited for proxy-based studies aimed at deciphering the causal mechanisms behind sapropel formation. Contrary to the more extreme but less well-dated Pliocene sapropels [*Passier et al.*, 1999], records for S5 can be placed on an absolute timescale [*Bar-Matthews et al.*, 2000], allowing the duration of processes to be more firmly assessed. Here we present new surface sediment coccolith results along with downcore coccolith results through S5 from a high sedimentation rate site (LC21) in the southeastern Aegean Sea. New and previously published data from LC21 [*Marino et al.*, 2007] are used to investigate the response of EMED nutrient budget and primary productivity in the upper water column to extensive freshwater-bound hydrographic changes.

2. Modern Water Mass and Nutrient Dynamics

[6] The Atlantic surface waters that enter the Mediterranean Sea through the Strait of Gibraltar subsequently flow into the EMED through the Strait of Sicily (Figure 1) and progressively gain heat and salt along this path [*Wüst*, 1961; *Malanotte-Rizzoli and Hecht*, 1988]. During winter-spring, sustained heat loss in the Rhodes cyclonic gyre leads to the formation of the Levantine Intermediate Water (LIW) [*Hecht et al.*, 1988; *Theocharis et al.*, 1999; *Zervakis et al.*, 2000; *Hecht and Gertman*, 2001]. LIW flows westward between 150 and 600 m water depth [*Pinardi and Masetti*, 2000] and pre-conditions deep water formation in the northern sectors of the basin [*Wu and Haines*, 1996].

[7] The EMED features a permanent nutricline between the density surfaces of 29.00–29.05 and 29.15 isopycnals throughout the basin [*Yılmaz and Tuğrul*, 1998], that is a depth ranging from 50 to 400 m in the southern Aegean Sea [*Theocharis et al.*, 1999]. Primary productivity is fuelled by entrainment of nutrients from lower layers, especially by wintertime vertical mixing [*Krom et al.*, 1992], and is higher in cyclonic regions such as, e.g., the Rhodes gyre, where doming of the isopycnals causes the nutricline to reach the base of the photic zone. Situated between the cyclonic Rhodes gyre to the east and the cyclonic Cretan gyre to the

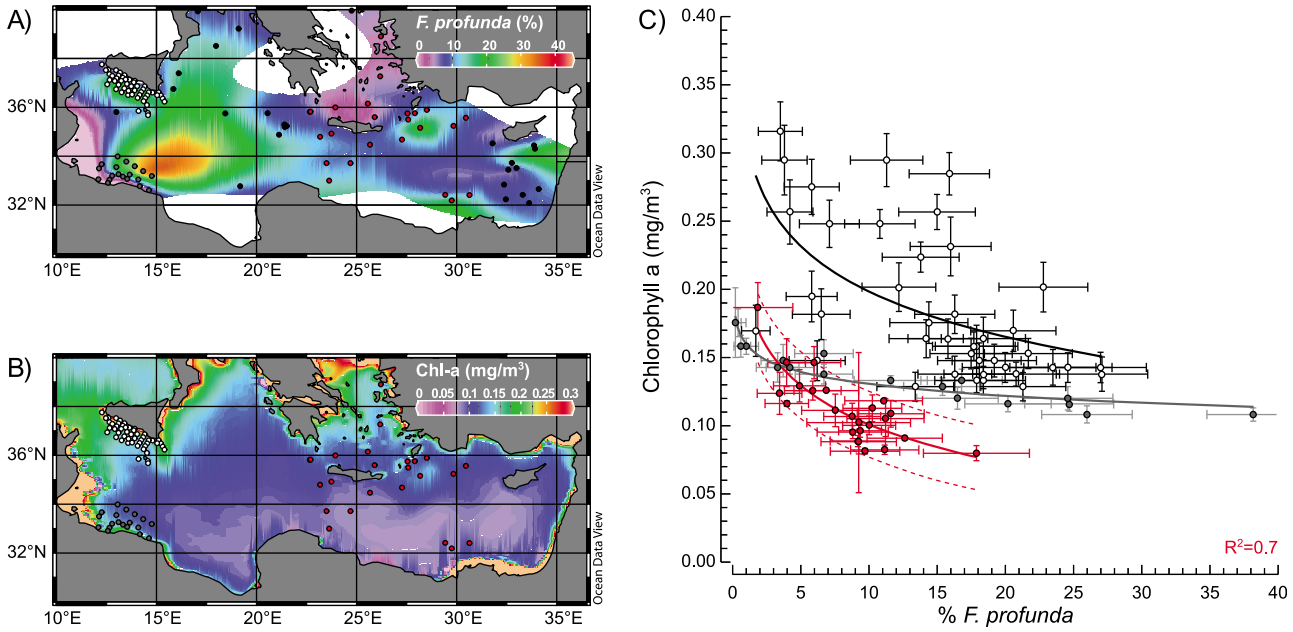

Figure 2. (a) Distribution map of the relative abundances of *F. profunda* in the surface sediment of the central and eastern Mediterranean Sea. (b) Distribution map of the averaged concentration of chlorophyll a (Chl-a) extracted from satellite imagery between 1996 and 2006 [*Feldman and McClain*, 2011]. The symbols are the same as in Figure 1. (c) Relation between the relative abundances of *F. profunda* and the surface concentration of Chl-a at the different sites: white circles, samples of the Sicily Strait [*Incarbona et al.*, 2008], gray circles, samples offshore Libya [*Incarbona et al.*, 2008]; and red circles, samples of the open eastern Mediterranean and southern Aegean Seas. The heavy black, gray and red lines depict the logarithmic regressions and the red dotted lines depict the 95% interval of confidence of our estimation, which takes into account for the respective uncertainties characterizing the Chl-a concentrations and the relative abundances of *F. profunda.* The vertical error bars correspond to 1σ and the horizontal error bars correspond to the 95% interval of confidence on the estimation of the relative abundances of *F. profunda.*

west (Figure 1), the site of core LC21 is characterized by a shallow nutricline which almost crops out in winter [see, e.g., *Theocharis et al.*, 1999, Figure 8b].

3. Material and Methods

[8] Sediment core LC21 (35°40′N, 26°35′E; 1522 m water depth, Figure 1) was recovered in 1995 by R/V *Marion Dufresne* [*Rothwell*, 1995]. The chronology used here for core LC21 through sapropel S5 follows *Marino et al.* [2007] and yields a temporal resolution of ~40 ± 20 yr cm^{-1} within S5.

[9] We analyzed S5, in core sections 5 and 6, at 2 cm spacing (102 samples) for the relative abundances of the coccolith species *Florisphaera profunda* and *Helicosphaera carteri*, and at coarser resolution (2 to 40 cm spacing) for absolute coccolith abundances. We also assessed the modern distribution of *F. profunda* in EMED surface sediments based on analyses of this taxon's relative abundances in 43 surface sediment samples retrieved during *R/V Meteor* cruises M40 leg 4 (1998), M50 leg 3 (2001) and M52 leg 2 (2002); and during the Biodeep01 and Biodeep02 cruises (1997) (Figure 2a). These new data supplement previously published data (124 samples in total, Table S1 in the auxiliary material).[1]

[1]Auxiliary materials are available in the HTML. doi:10.1029/2012PA002288.

3.1. Calcareous Nannofossil Analyses

[10] Quantitative analyses of calcareous nannofossil abundances were performed with a polarized light microscope with ×1000 magnification. The smear slides were prepared following standard procedures on the <63 μm sediment fraction for both core LC21 and surface sediment samples. An average of ~680 (surface sediments) and ~350 (LC21 downcore record) coccolith specimen were counted for each sample.

[11] Absolute coccolith abundances were estimated for 10 samples of LC21 quantifying the number of coccoliths in a portion of the filtered sediment samples [*Lototskaya et al.*, 1998]. Samples were prepared as follows: about 0.01 g of sediment was diluted in 100 ml of tap-water and placed in an ultrasonic bath few seconds in order to disaggregate it. The samples were then filtered through a Milipore membrane (47 mm diameter, 0.45 μm pore size) using a low pressure vacuum pump to obtain even distribution of the particles on the filter. The filter was oven-dried at 40°C for 1 h. Finally, a quarter of the filter was mounted with Canadian balsam to make a permanent slide.

3.2. Chlorophyll a (Chl-a) Concentrations

[12] The annual composite data of chlorophyll-a (Chl-a) concentration used to calibrate our coccolith-based proxies (Figure 2b), were extracted from the NASA Ocean Color and Temperature Scanner (OCTS), the Coastal Zone Color Scanner (CZCS) experiment and the Sea-viewing Wide

Field-of-view Sensor (SeaWiFS) project, in order to cover the period from 1986 to 2002 that corresponds to the different oceanographic cruises considered here (Table S1 in the auxiliary material). The Chl-a data are distributed as a Level-3 Binned file product (BIN), reprocessing No. 5, October 2011 [*Feldman and McClain*, 2011]. The annual composites were downloaded from the http://oceancolor.gsfc.nasa.gov/ website in Hierarchical Data Format (HDF). The images have a resolution of 9 km^2 (4320 × 2160 pixels) and were analyzed using SeaDAS [*Baith et al.*, 2001]. Information was extracted from the pixels closest to the location of the surface sediment sample sites, and for each sample we averaged the data of the year of the cruise and the year just before.

4. Ecology of the Selected Coccolithophore Species in the Mediterranean Sea

[13] *Florisphaera profunda* inhabits the lower photic zone [*Okada and Honjo*, 1973; *Honjo and Okada*, 1974; *Okada and McIntyre*, 1977; *Matsuoka and Okada*, 1989; *Molfino and McIntyre*, 1990; *Ujiie et al.*, 1991]. High relative abundances of this taxon are diagnostic of the presence of a well-developed DCM, generally associated with stratified and nutrient-depleted waters in the upper photic zone. This view is corroborated by recent surface water and sediment-trap studies on coccolithophore distribution and export production in the EMED [*Malinverno et al.*, 2003, 2009].

[14] These ecological features make *F. profunda* particularly well suited to document temporal changes in the development of the DCM and to qualitatively infer the depth of the nutricline [*Okada and Honjo*, 1973; *Molfino and McIntyre*, 1990; *Castradori*, 1993; *Beaufort et al.*, 1997]. In addition, relative abundances of *F. profunda* increase (decrease) when the upper photic zone is impoverished (replenished) in nutrients [*Beaufort et al.*, 1997; *Incarbona et al.*, 2008]. We reconstruct past dynamics of the nutricline within the photic zone in the southeastern Aegean Sea from down-core records of *F. profunda* percentages. Additional support to this reconstruction is provided by mapping the distribution of *F. profunda* in the EMED surface sediments at several locations (Figure 2a), for which modern (satellite-derived) estimates of Chl-a concentrations at the sea surface are available (Figure 2b).

[15] A second species we focus on is *Helicosphaera carteri*, which is considered as a coastal taxon, indicative of moderately elevated nutrient conditions and turbidity [*Giraudeau*, 1992; *Ziveri et al.*, 1995, 2000; *Colmenero-Hidalgo et al.*, 2004; *Ziveri et al.*, 2004; *Malinverno et al.*, 2009]. Previous work has attributed high abundances of *H. carteri* to fresher and probably more turbid surface waters in the Alboran Sea [*Colmenero-Hidalgo et al.*, 2004] and the Adriatic Sea (during S5) [*Narciso et al.*, 2010].

5. Results

5.1. Proxy Validation: Relative Abundances of *F. profunda* in the Central and Eastern Mediterranean Sea Versus Chl-a Concentrations

[16] In surface samples from the central and eastern Mediterranean Sea, the relative abundances of *F. profunda* range between 0.20% and 38.15% (N = 124, average = 11.86, σ = 7.27) (Figure 2a). *Florisphaera profunda* percentages remain generally in the same order of magnitude throughout the study area with the exception of the southern Aegean Sea and offshore Libya, where values are lower due to shallower water depth (Figure 2a), in line with previous studies [*Incarbona et al.*, 2008]. We note an exponential anticorrelation *between F. profunda* percentages and surface water Chl-a concentrations (Figure 2c) throughout the EMED:

$$\text{Chl-a} = -0.041 \times \ln(\%\ F.\,profunda) + 0.196 \cdot \left(R^2 = 0.70, N = 24, \sigma = 0.018\right) \quad (1)$$

This supports previous studies carried out in the Mediterranean Sea [*Incarbona et al.*, 2008] as well as in other regions of the world ocean [*Beaufort et al.*, 1997, 2001, 2003], pointing to an exponential increase of *F. profunda* percentages when primary productivity of the surface waters decreases, or – in other words – when the locus of productivity shifts to subsurface.

5.2. The LC21 Downcore Record

[17] Figure 3 shows our downcore coccolith records in LC21 along with other previously reported geochemical and sedimentary data from the same site [*Marino et al.*, 2007]. *Florisphaera profunda* percentages exhibit relatively low values in the pre- and post-sapropel sections (<20%), an abrupt increase up to ~58% prior to the onset of the anoxic sedimentation, and values between 20 and 38% (the latter value corresponding to a distinct peak at ~122.2 ka BP) throughout the remainder of the sapropel event (Figure 3a). The LC21 *H. carteri* percentages likewise display higher values during the sapropel event and lower values before and after S5 (Figure 3b). After an abrupt increase roughly coincident with the aforementioned *F. profunda* peak, the S5 is characterized by a long-term decrease punctuated by several short-term peaks, to eventually reach pre-sapropel values in step with the cessation of the anoxic sedimentation. The absolute abundance of coccoliths (Figure 3a) displays opposing patterns with respect to both *F. profunda* and *H. carteri* profiles in that it is higher in the non-sapropel intervals and lower during S5.

6. Discussion

[18] The high *F. profunda* percentages within sapropel S5 in southeastern Aegean core LC21 (Figure 3a) agree with previous observations of enhanced abundances of this taxon in several eastern Mediterranean sapropels, relative to non-sapropel intervals [*Castradori*, 1993; *Negri et al.*, 1999; *Triantaphyllou et al.*, 2010; *Incarbona et al.*, 2011]. The evidence from LC21 supports the initial foraminifer-based hypothesis of a strong DCM during the intensively developed sapropel S5 [*Rohling and Gieskes*, 1989], as opposed to generally productive conditions in the upper photic zone. The co-registered nature and the high temporal resolution of the LC21 records allow unambiguous documentation of the timing relationships between freshwater-bound hydrographic changes in the upper water column, development of

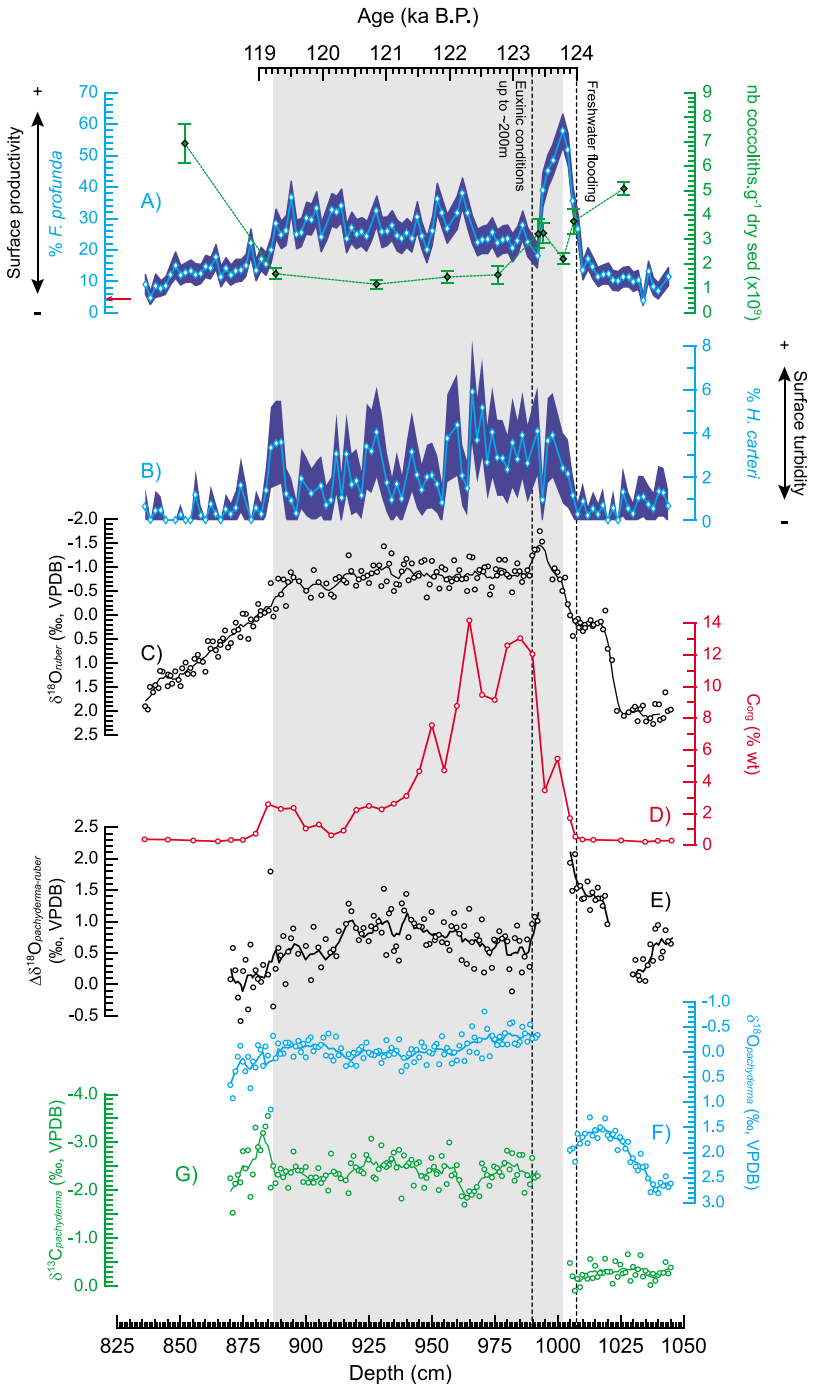

Figure 3. Nannofloral and geochemical proxies along core LC21. (a) Blue line and associated diamonds symbols represent the relative abundances of *F. profunda.* The dark blue shaded area gives the 95% interval of confidence of the estimation of the relative abundances of *F. profunda.* The absolute concentrations of coccoliths are depicted by the dotted green line and associated diamonds symbols. The error bar, represent the 1σ standard error (calculated from 5 to 15 different counts for the same sample). The red arrow along the *y* axis depicts the modern values around the LC21 site for the relative abundances of *F. profunda.* (b) Relative abundances of *H. carteri*, the dark blue shaded area gives the 95% interval of confidence of the estimation of the relative abundances of *H. carteri*, (c) $\delta^{18}O_{ruber}$ (black circles) and $\delta^{18}O_{ruber}$ loess smoothed (heavy black line), (d) organic carbon (C_{org}) content, (e) $\Delta\delta^{18}O_{pachyderma\text{-}ruber}$ (black circles) and $\Delta\delta^{18}O_{pachyderma\text{-}ruber}$ loess smoothed (heavy black line), (f) $\delta^{18}O_{pachyderma}$ (blue circles) and $\delta^{18}O_{pachyderma}$ loess smoothed (heavy blue line), and (g) $\delta^{13}C_{pachyderma}$ (green circles) and $\delta^{13}C_{pachyderma}$ loess smoothed (heavy green line) [*Marino et al.*, 2007].

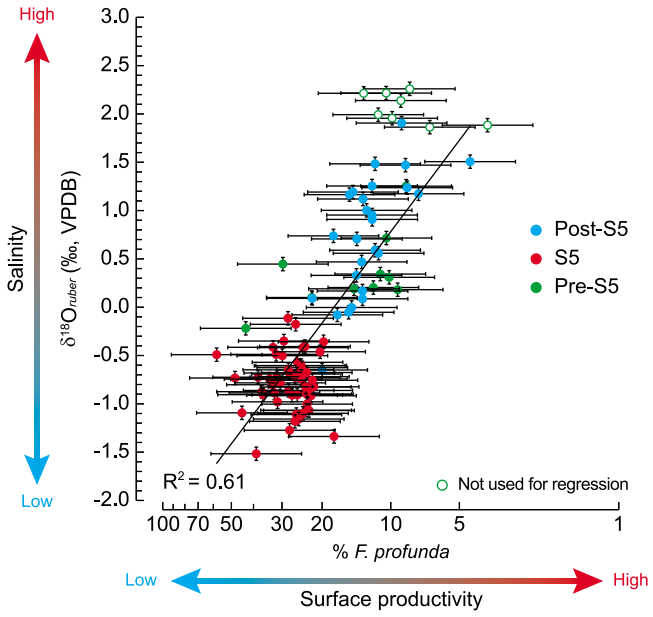

Figure 4. Comparison of the surface proxy derived from the relative abundances of *F. profunda* with the planktonic foraminiferal geochemical proxies. Relative abundances of *F. profunda*, here in logarithmic scale as depicted in equation (1), versus the $\delta^{18}O_{ruber}$. The vertical error bars represent the external precision and the horizontal error bars the 1σ (related to values calculated from equation (1)). We prefer to discard the 8 first pre-S5 samples (open green circles) as the $\delta^{18}O_{ruber}$ values have the icevolume imprint of the Termination II.

the DCM and onset of the organic-rich sedimentation in the southeastern Aegean Sea.

6.1. Freshwater Flooding, Development of the DCM and Dynamics of the Nutricline

[19] The LC21 records reveal that the abrupt increase of *F. profunda* and *H. carteri* percentages and the decrease in the total coccolith abundances at ~124 ka coincides with the first half of the ~1.7‰ decrease in $\delta^{18}O_{ruber}$ (Figure 3c), which preceded by a few decades [*Marino et al.*, 2007] the onset of the C_{org} deposition at the same site (Figure 3d). The negative $\delta^{18}O_{ruber}$ shift testifies to pronounced sea surface freshening prior to S5 deposition [*Marino et al.*, 2007], while the prominent *F. profunda* peak marks the development of a productive DCM in the subsurface. The remarkable synchroneity (within the multidecadal resolution of the records) of these changes highlights a strong coupling between freshwater-bound hydrographic changes at the sea surface and subsurface productivity increase in the southeastern Aegean Sea. A sharp reduction of the surface buoyancy loss likely reduced deep convective mixing and amplified vertical stratification between surface and subsurface waters, as exemplified by steep oxygen isotope gradients ($\Delta\delta^{18}O$, Figure 3e) between subsurface-dwelling *Neogloboquadrina pachyderma* (dextral) (Figure 3f) and surface-dwelling *Globigerinoides ruber* (Figure 3c) [cf. *Rohling et al.*, 2004, 2006].

[20] It has been suggested that these developments caused the LIW to shoal [*Rohling*, 1994; *Myers et al.*, 1998; *Rohling et al.*, 2006], promoting enhanced upward advection of nutrients [*Rohling and Gieskes*, 1989] that fuelled a productive DCM below a strong salinity gradient (halocline). Nutrient utilization within the DCM and the virtual absence of mixing in the upper water column [*Rohling et al.*, 2006; *Marino et al.*, 2007] would nutrient-starve the surface system above it [*Sachs and Repeta*, 1999], consistent with the drop in overall coccolith concentrations in our records. Additional insights into the depth of the DCM prior to S5 deposition in LC21 are provided by the contemporaneous increase of *H. carteri*, which suggests increased turbidity of surface waters at this location. This would have inhibited light penetration (hence photosynthesis) at depth, implying that the nutricline was positioned in the subsurface yet at relatively shallow levels in the photic layer.

[21] The sharp C_{org} increase to values higher than 13% at ~123.3 coincided with an expansion of euxinic conditions from the bottom to ~200 m depth and with the accumulation of respiration products at the base of the photic zone (very low $\delta^{13}C_{pachyderma}$ in Figure 3g) [*Marino et al.*, 2007]. Oxygen-starved conditions would have promoted extensive denitrification [*Krom et al.*, 2010] and phosphorous regeneration [*Slomp et al.*, 2002], thereby enhancing the nutrient availability within the water column. It seems therefore surprising that the *F. profunda* percentages decreased considerably at 123.3 ka and remained generally low throughout S5 (yet still higher by ~15% than in non-S5 intervals). There is a possibility that during S5 the DCM was dominated by phytoplankton groups other than coccoliths, e.g., diatoms [*Kemp et al.*, 1999]. This is supported by the low coccolith concentrations in LC21 (Figure 3a) and would also agree with the lowered $CaCO_3$ levels generally found in the EMED sapropels [*Van Os et al.*, 1994; *Reitz and de Lange*, 2006]. Alternatively, the sharp reduction of the vertical stratification (erosion of the halocline) that we observe at ~123.3 (low $\Delta\delta^{18}O$, Figure 3e), via downward diffusive mixing [*Casford et al.*, 2002] of the freshening signal (low *N. pachyderma* $\delta^{18}O$, Figure 3f) may have inhibited the concentration of nutrients near the base of the photic zone and, in turn, decreased productivity within the DCM.

[22] The very low percentages of *F. profunda* and high coccolith concentrations (Figure 3a) in the non-S5 sections point to an oligotrophic photic zone with most of the primary production focused within its upper part. During both the pre- and post S5 intervals, and similar to the present-day EMED, the upper water column was homogenized (low $\Delta\delta^{18}O$), with well-ventilated subthermocline waters [*Pierre*, 1999; *Rohling et al.*, 2006]. The nutricline likely was positioned below the photic zone with the surface primary productivity resulting, from upward mixing and entrainment of thermocline waters during the winter season [*Krom et al.*, 2003]. At ~119 ka the *N. pachyderma* $\delta^{13}C$ decreased, in apparent disagreement with the proposed return to pre-S5 conditions. This may be explained by upward admixture of old deep waters, laden with isotopically light (respired) CO_2, due to the resumption of deep-water formation. It is interesting that, although these developments would have

presumably lifted remineralized nutrients toward the photic zone [*Stratford and Haines*, 2002], the low *F. profunda* percentages suggest no productivity increase in the DCM during this period. This evidence emphasizes that the freshwater-induced shoaling of the pycnocline and the development of a distinct halocline underneath a freshened surface layer are fundamental ingredients to develop a nutrient-replete DCM while the sea surface experiences nutrient-starvation.

6.2. Impacts of the Hydrographic and Productivity Changes on the Development of Anoxic Conditions in the Eastern Mediterranean Sea

[23] The LC21 records presented here provide the first direct evidence that, prior to the deposition of the last interglacial sapropel S5, the nutricline abruptly (within less than a century) shoaled within the photic layer and that this change occurred in concert with a series of major hydrographic reorganizations initiated by massive [*Rohling et al.*, 2002] monsoon-fuelled freshwater discharge along the North African margin [*Rohling et al.*, 2002; *Osborne et al.*, 2008, 2010]. Two additional lines of evidence support the tight coupling between freshwater perturbation in the EMED and the vertical migration of the nutricline in the upper water column. First, the distinct increase of *F. profunda* percentages at ~122.2 ka BP in LC21 (see Figure S1 in the auxiliary material) coincides with the reactivation of the excess monsoon discharge route through the Libyan Sahara [*Osborne et al.*, 2008] into the EMED [*Rohling et al.*, 2002]. Second, $\delta^{18}O_{ruber}$ and F. *profunda* percentages strongly covary in LC21 (Figure 4). Accordingly, curtailment of the EMED deep ventilation [*Marino et al.*, 2007] and increased productivity in the DCM (this study) can both be seen as abrupt responses of the EMED thermohaline cells and of the vertical flux of nutrients (and their subsequent utilization) to the orbitally driven [*Revel et al.*, 2010; *Ziegler et al.*, 2010] monsoon floods.

[24] The enhanced C_{org} preservation promoted by seafloor anoxia is unlikely to account alone for the abrupt transition from C_{org}-depleted to C_{org}-enriched sediments in the EMED, let alone for the remarkably high C_{org} levels (up to ~14%) found in the southeastern Aegean sediments during S5 (Figure 3d) [*Marino et al.*, 2007]. The particularly high C_{org} values in LC21 and at other locations throughout the EMED during S5 [*Struck et al.*, 2001; *Rohling et al.*, 2006] are contrasted with moderate C_{org} levels (~2–3%) found in the Aegean Sea [*Mercone et al.*, 2001; *Thomson et al.*, 2004] and in the EMED [*De Lange et al.*, 2008] during S1 and in other Late Pleistocene sapropels [*Kallel et al.*, 2000]. We suggest that the elevated C_{org} levels of the last interglacial sapropel event require a concomitant increase in the export flux of organic matter to the seafloor. Reconstruction based on coccoliths (this study) and on diatoms [*Kemp et al.*, 1999] prove that prior to and during S5 deposition, an increased C_{org} export to the deep sea likely resulted from the development of a productive DCM in the EMED subsurface. By contrast, the weakly developed S1 features lower *F. profunda* percentages [*Negri et al.*, 1999; *Thomson et al.*, 2004; *Triantaphyllou et al.*, 2009] and a lack of diatoms [*Boere et al.*, 2011]. Hence, the amount of freshwater discharged and its associated hydrographic changes, together with the advection across the upper water column of nutrients that are regenerated under oxygen-starved conditions [*Slomp et al.*, 2002; *Krom et al.*, 2010], modulate the magnitude of C_{org} burial in the EMED sediments during sapropel formation.

7. Conclusions

[25] We presented new coccolith records (*F. profunda* and *H. carteri* percentages, coccolith concentrations) that document in high temporal detail the primary productivity and turbidity changes prior to, during, and after the deposition of the last interglacial sapropel S5 in the southeastern Aegean Sea core LC21. The (negative) exponential relationship between *F. profunda* percentages and satellite-derived Chl-a concentrations at 24 locations in the EMED supports the employment of downcore relative abundances of this taxon to reconstruct past productivity patterns in LC21.

[26] Comparison of our coccolith records with the co-registered planktonic foraminiferal stable isotopes from the southeastern Aegean Sea reveals that the onset of the sea surface freshening prior to S5 deposition [*Marino et al.*, 2007] was accompanied by an abrupt shift toward higher turbidity and lower primary productivity conditions in the surface waters, while a productive DCM developed in the subsurface. The remarkable synchroneity of these developments points to a strong sensitivity and instantaneous response (within less than a century) of the vertical fluxes and utilization of nutrients to freshwater perturbation in the EMED. Specifically, the onset of major monsoon-fuelled freshwater flooding within the last interglacial period [*Rohling et al.*, 2002, 2004] initiated a series of hydrographic adjustments that rapidly culminated in the isolation of a nutrient-starved surface layer from a nutrient-replete DCM.

[27] We speculate that the permanent cyclonic circulation at the LC21 core site and the associated "doming" of the isopycnals caused the nutricline to shoal well within the photic layer during the S5. This fuelled a DCM that was possibly more productive than in other sectors of the EMED featuring different circulation regimes (e.g., close to anticyclonic gyres), thereby (partly) explaining the very low subsurface $\delta^{13}C$ values and the rapid upward progression of the euxinic conditions previously documented in LC21 [*Marino et al.*, 2007]. These features agree well with the enhanced denitrification in the water column [*Krom et al.*, 2010] and sediments and with the phosphorus recycling [*Slomp et al.*, 2002] proposed for the EMED during sapropel formation.

[28] **Acknowledgments.** This research is made possible thanks to the support from the EU FP7 MedSeA project (grant agreement 265103), the Spanish Ministry of Science and Innovation cofunded by the European Fund, and FP6 MarinERA (CGL2009-10806). We thank Kay Emeis and Alessandro Incarbona for providing the surface sediment samples used in this study and one anonymous reviewer and Christopher Charles (Editor) for their constructive comments. G.M. acknowledges support from the Universitat Autònoma de Barcelona (postdoctoral research grant PS-688-01/08). E.J.R. acknowledges support from a Royal Society-Wolfson Research Merit Award and from UK Natural Environment Research Council Project NE/E01531X/1.

References

Baith, K., R. Lindsay, and G. Fu (2001), Data analysis system developed for ocean color satellite sensors, *Eos Trans. AGU*, *82*(18), 202, doi:10.1029/01EO00109.

Bar-Matthews, M., A. Ayalon, and A. Kaufman (2000), Timing and hydrological conditions of Sapropel events in the Eastern Mediterranean, as

evident from speleothems, Soreq cave, Israel, *Chem. Geol.*, *169*(1–2), 145–156, doi:10.1016/S0009-2541(99)00232-6.

Beaufort, L., Y. Lancelot, P. Camberlin, O. Cayre, E. Vincent, F. Bassinot, and L. Labeyrie (1997), Insolation cycles as a major control of equatorial Indian Ocean primary production, *Science*, *278*(5342), 1451–1454, doi:10.1126/science.278.5342.1451.

Beaufort, L., T. de Garidel-Thoron, A. C. Mix, and N. G. Pisias (2001), ENSO-like forcing on oceanic primary production during the Late Pleistocene, *Science*, *293*(5539), 2440–2444, doi:10.1126/science.293.5539.2440.

Beaufort, L., T. de Garidel-Thoron, B. Linsley, D. Oppo, and N. Buchet (2003), Biomass burning and oceanic primary production estimates in the Sulu Sea area over the last 380 kyr and the East Asian monsoon dynamics, *Mar. Geol.*, *201*(1–3), 53–65, doi:10.1016/S0025-3227(03)00208-1.

Boere, A. C., W. I. C. Rijpstra, G. J. De Lange, J. S. Sinninghe, É. Damst, and M. J. L. Coolen (2011), Preservation potential of ancient plankton DNA in Pleistocene marine sediments, *Geobiology*, *9*(5), 377–393, doi:10.1111/j.1472-4669.2011.00290.x.

Calvert, S. E., B. Nielsen, and M. R. Fontugne (1992), Evidence from nitrogen isotope ratios for enhanced productivity during formation of Eastern Mediterranean sapropels, *Nature*, *359*(6392), 223–225, doi:10.1038/359223a0.

Casford, J. S. L., E. J. Rohling, R. Abu-Zied, S. Cooke, C. Fontanier, M. Leng, and V. Lykousis (2002), Circulation changes and nutrient concentrations in the late Quaternary Aegean Sea: A nonsteady state concept for sapropel formation, *Paleoceanography*, *17*(2), 1024, doi:10.1029/2000PA000601.

Casford, J. S. L., E. J. Rohling, R. H. Abu-Zied, C. Fontanier, F. J. Jorissen, M. J. Leng, G. Schmiedl, and J. Thomson (2003), A dynamic concept for eastern Mediterranean circulation and oxygenation during sapropel formation, *Palaeogeogr. Palaeoclimatol. Palaeoecol.*, *190*, 103–119, doi:10.1016/S0031-0182(02)00601-6.

Castradori, D. (1993), Calcareous nannofossils and the origin of eastern Mediterranean sapropels, *Paleoceanography*, *8*(4), 459–471, doi:10.1029/93PA00756.

Colmenero-Hidalgo, E., J.-A. Flores, F. J. Sierro, M. Á. Bárcena, L. Löwemark, J. Schönfeld, and J. O. Grimalt (2004), Ocean surface water response to short-term climate changes revealed by coccolithophores from the Gulf of Cadiz (NE Atlantic) and Alboran Sea (W Mediterranean), *Palaeogeogr. Palaeoclimatol. Palaeoecol.*, *205*(3–4), 317–336, doi:10.1016/j.palaeo.2003.12.014.

Cramp, A., and G. O'Sullivan (1999), Neogene sapropels in the Mediterranean: A review, *Mar. Geol.*, *153*(1–4), 11–28, doi:10.1016/S0025-3227(98)00092-9.

D'Ortenzio, F., and M. Ribera d'Alcalà (2009), On the trophic regimes of the Mediterranean Sea: A satellite analysis, *Biogeosciences*, *6*(2), 139–148, doi:10.5194/bg-6-139-2009.

De Lange, G. J., and H. L. ten Haven (1983), Recent sapropel formation in the eastern Mediterranean, *Nature*, *305*(5937), 797–798, doi:10.1038/305797a0.

De Lange, G. J., J. Thomson, A. Reitz, C. P. Slomp, M. Speranza Principato, E. Erba, and C. Corselli (2008), Synchronous basin-wide formation and redox-controlled preservation of a Mediterranean sapropel, *Nat. Geosci.*, *1*(9), 606–610, doi:10.1038/ngeo283.

Feldman, G. C., and C. R. McClain (2011), Ocean Color Web, CZCS, OCTS and SeaWiFS Reprocessing 5, report, edited by N. Kuring and S. W. Bailey, NASA Goddard Space Flight Cent., Greenbelt, Md.

Giraudeau, J. (1992), Distribution of Recent Nannofossils beneath the Benguela System - Southwest African Continental-Margin, *Mar. Geol.*, *108*(2), 219–237, doi:10.1016/0025-3227(92)90174-G.

Hecht, A., and I. Gertman (2001), Physical features of the eastern Mediterranean resulting from the integration of POEM data with Russian Mediterranean Cruises, *Deep Sea Res., Part I*, *48*(8), 1847–1876, doi:10.1016/S0967-0637(00)00113-8.

Hecht, A., N. Pinardi, and A. R. Robinson (1988), Currents, water masses, eddies and jets in the Mediterranean Levantine Basin, *J. Phys. Oceanogr.*, *18*(10), 1320–1353, doi:10.1175/1520-0485(1988)018<1320:CWMEAJ>2.0.CO;2.

Honjo, S., and H. Okada (1974), Community structure of coccolithophores in the photic layer of the mid-Pacific, *Micropaleontology*, *20*(2), 209–230, doi:10.2307/1485061.

Ignatiades, L., O. Gotsis-Skretas, K. Pagou, and E. Krasakopoulou (2009), Diversification of phytoplankton community structure and related parameters along a large-scale longitudinal east–west transect of the Mediterranean Sea, *J. Plankton Res.*, *31*(4), 411–428, doi:10.1093/plankt/fbn124.

Incarbona, A., et al. (2008), Calcareous nannofossil surface sediment assemblages from the Sicily Channel (central Mediterranean Sea): Palaeoceanographic implications, *Mar. Micropaleontol.*, *67*(3–4), 297–309, doi:10.1016/j.marmicro.2008.03.001.

Incarbona, A., P. Ziveri, N. Sabatino, D. S. Manta, and M. Sprovieri (2011), Conflicting coccolithophore and geochemical evidence for productivity levels in the Eastern Mediterranean sapropel S1, *Mar. Micropaleontol.*, *81*(3–4), 131–143, doi:10.1016/j.marmicro.2011.09.003.

Kallel, N., J. C. Duplessy, L. Labeyrie, M. Fontugne, M. Paterne, and M. Montacer (2000), Mediterranean pluvial periods and sapropel formation over the last 200 000 years, *Palaeogeogr. Palaeoclimatol. Palaeoecol.*, *157*(1–2), 45–58, doi:10.1016/S0031-0182(99)00149-2.

Kemp, A. E. S., R. B. Pearce, I. Koizumi, J. Pike, and S. J. Rance (1999), The role of mat-forming diatoms in the formation of Mediterranean sapropels, *Nature*, *398*, 57–61.

Krom, M. D., N. Kress, S. Brenner, and L. I. Gordon (1991), Phosphorus limitation of primary production in the eastern Mediterranean Sea, *Limnol. Oceanogr.*, *36*, 424–432, doi:10.4319/lo.1991.36.3.0424.

Krom, M. D., S. Brenner, N. Kress, A. Neori, and L. I. Gordon (1992), Nutrient dynamics and new production in a warm-core eddy from the Eastern Mediterranean Sea, *Deep Sea Res., Part A*, *39*(3–4), 467–480, doi:10.1016/0198-0149(92)90083-6.

Krom, M. D., S. Groom, and T. Zohary (2003), The Eastern Mediterranean, in *Biogeochemistry of Marine Systems*, edited by K. D. Black and G. B. Shimmield, pp. 91–126, CRC Press, Boca Raton, Fla.

Krom, M. D., K. C. Emeis, and P. Van Cappellen (2010), Why is the Eastern Mediterranean phosphorus limited?, *Prog. Oceanogr.*, *85*(3–4), 236–244, doi:10.1016/j.pocean.2010.03.003.

Lototskaya, A., P. Ziveri, G. M. Ganssen, and J. E. van Hinte (1998), Calcareous nannofloral response to Termination II at 45°N, 25°W (northeast Atlantic), *Mar. Micropaleontol.*, *34*(1–2), 47–70, doi:10.1016/S0377-8398(98)00005-X.

Malanotte-Rizzoli, P., and A. Hecht (1988), Large-scale properties of the Eastern Mediterranean: A review, *Oceanol. Acta*, *11*(4), 323–335.

Malinverno, E., P. Ziveri, and C. Corselli (2003), Coccolithophorid distribution in the Ionian Sea and its relationship to eastern Mediterranean circulation during late fall to early winter 1997, *J. Geophys. Res.*, *108*(C9), 8115, doi:10.1029/2002JC001346.

Malinverno, E., M. V. Triantaphyllou, S. Stavrakakis, P. Ziveri, and V. Lykousis (2009), Seasonal and spatial variability of coccolithophore export production at the South–Western margin of Crete (Eastern Mediterranean), *Mar. Micropaleontol.*, *71*(3–4), 131–147, doi:10.1016/j.marmicro.2009.02.002.

Marino, G., E. J. Rohling, W. I. C. Rijpstra, F. Sangiorgi, S. Schouten, and J. S. S. Damsté (2007), Aegean Sea as driver of hydrographic and ecological changes in the eastern Mediterranean, *Geology*, *35*(8), 675–678, doi:10.1130/G23831A.1.

Marino, G., E. J. Rohling, F. Sangiorgi, A. Hayes, J. L. Casford, A. F. Lotter, M. Kucera, and H. Brinkhuis (2009), Early and middle Holocene in the Aegean Sea: Interplay between high and low latitude climate variability, *Quat. Sci. Rev.*, *28*(27–28), 3246–3262, doi:10.1016/j.quascirev.2009.08.011.

Matsuoka, H., and H. Okada (1989), Quantitative analysis of quaternary nannoplankton in the subtropical northwestern Pacific Ocean, *Mar. Micropaleontol.*, *14*(1–3), 97–118, doi:10.1016/0377-8398(89)90033-9.

Mercone, D., J. Thomson, R. H. Abu-Zied, I. W. Croudace, and E. J. Rohling (2001), High-resolution geochemical and micropalaeontological profiling of the most recent eastern Mediterranean sapropel, *Mar. Geol.*, *177*(1–2), 25–44, doi:10.1016/S0025-3227(01)00122-0.

Molfino, B., and A. McIntyre (1990), Precessional forcing of nutricline dynamics in the equatorial Atlantic, *Science*, *249*(4970), 766–769, doi:10.1126/science.249.4970.766.

Myers, P. G., K. Haines, and E. J. Rohling (1998), Modeling the paleocirculation of the Mediterranean: The Last Glacial Maximum and the Holocene with emphasis on the formation of sapropel S_1, *Paleoceanography*, *13*(6), 586–606, doi:10.1029/98PA02736.

Narciso, À., J.-A. Flores, M. Cachão, F. J. Sierro, E. Colmenero-Hidalgo, A. Piva, and A. Asioli (2010), Sea surface dynamics and coccolithophore behaviour during sapropel deposition of Marine Isotope Stage 7, 6 and 5 in the Western Adriatic sea, *Rev. Esp. Micropaleontol.*, *42*(3), 345–358.

Negri, A., L. Capotondi, and J. Keller (1999), Calcareous nannofossils, planktonic foraminifera and oxygen isotopes in the late Quaternary sapropels of the Ionian Sea, *Mar. Geol.*, *157*(1–2), 89–103, doi:10.1016/S0025-3227(98)00135-2.

Negri, A., A. Ferretti, T. Wagner, and P. A. Meyers (2009), Phanerozoic organic-carbon-rich marine sediments: Overview and future research challenges, *Palaeogeogr. Palaeoclimatol. Palaeoecol.*, *273*(3–4), 218–227, doi:10.1016/j.palaeo.2008.10.002.

Okada, H., and S. Honjo (1973), The distribution of oceanic coccolithophorids in the Pacific, *Deep Sea Res., Part I*, *20*, 355–374.

Okada, H., and A. McIntyre (1977), Modern coccolithophores of the Pacific and North Atlantic oceans, *Micropaleontology*, *23*(1), 1–54, doi:10.2307/1485309.

Osborne, A. H., D. Vance, E. J. Rohling, N. Barton, M. Rogerson, and N. Fello (2008), A humid corridor across the Sahara for the migration of early modern humans out of Africa 120,000 years ago, *Proc. Natl. Acad. Sci. U. S. A.*, *105*(43), 16,444–16,447, doi:10.1073/pnas.0804472105.

Osborne, A. H., G. Marino, D. Vance, and E. J. Rohling (2010), Eastern Mediterranean surface water Nd during Eemian sapropel S5: Monitoring northerly (mid-latitude) versus southerly (sub-tropical) freshwater contributions, *Quat. Sci. Rev.*, *29*(19–20), 2473–2483, doi:10.1016/j.quascirev.2010.05.015.

Passier, H. F., H.-J. Bosch, I. A. Nijenhuis, L. J. Lourens, M. E. Bottcher, A. Leenders, J. S. S. Damste, G. J. de Lange, and J. W. Leeuw (1999), Sulphidic Mediterranean surface waters during Pliocene sapropel formation, *Nature*, *397*(6715), 146–149, doi:10.1038/16441.

Pierre, C. (1999), The oxygen and carbon isotope distribution in the Mediterranean water masses, *Mar. Geol.*, *153*(1–4), 41–55, doi:10.1016/S0025-3227(98)00090-5.

Pinardi, N., and E. Masetti (2000), Variability of the large scale general circulation of the Mediterranean Sea from observations and modelling: A review, *Palaeogeogr. Palaeoclimatol. Palaeoecol.*, *158*(3–4), 153–173, doi:10.1016/S0031-0182(00)00048-1.

Reitz, A., and G. J. de Lange (2006), Abundant Sr-rich aragonite in eastern Mediterranean sapropel S1: Diagenetic vs. detrital/biogenic origin, *Palaeogeogr. Palaeoclimatol. Palaeoecol.*, *235*(1–3), 135–148, doi:10.1016/j.palaeo.2005.10.024.

Revel, M., E. Ducassou, F. E. Grousset, S. M. Bernasconi, S. Migeon, S. Revillon, J. Mascle, A. Murat, S. Zaragosi, and D. Bosch (2010), 100,000 years of African monsoon variability recorded in sediments of the Nile margin, *Quat. Sci. Rev.*, *29*(11–12), 1342–1362, doi:10.1016/j.quascirev.2010.02.006.

Rohling, E. J. (1994), Review and new aspects concerning the formation of eastern Mediterranean sapropels, *Mar. Geol.*, *122*(1–2), 1–28, doi:10.1016/0025-3227(94)90202-X.

Rohling, E. J., and H. L. Bryden (1992), Man-induced salinity and temperature increases in Western Mediterranean Deep Water, *J. Geophys. Res.*, *97*(C7), 11,191–11,198, doi:10.1029/92JC00767.

Rohling, E. J., and W. W. C. Gieskes (1989), Late Quaternary changes in Mediterranean intermediate water density and formation rate, *Paleoceanography*, *4*(5), 531–545, doi:10.1029/PA004i005p00531.

Rohling, E. J., et al. (2002), African monsoon variability during the previous interglacial maximum, *Earth Planet. Sci. Lett.*, *202*(1), 61–75, doi:10.1016/S0012-821X(02)00775-6.

Rohling, E. J., et al. (2004), Reconstructing past planktic foraminiferal habitats using stable isotope data: A case history for Mediterranean sapropel S5, *Mar. Micropaleontol.*, *50*(1–2), 89–123, doi:10.1016/S0377-8398(03)00068-9.

Rohling, E. J., E. C. Hopmans, and J. S. Sinninghe Damsté (2006), Water column dynamics during the last interglacial anoxic event in the Mediterranean (sapropel S5), *Paleoceanography*, *21*, PA2018, doi:10.1029/2005PA001237.

Rossignol-Strick, M., W. Nesteroff, P. Olive, and C. Vergnaud-Grazzini (1982), After the deluge: Mediterranean stagnation and sapropel formation, *Nature*, *295*(5845), 105–110, doi:10.1038/295105a0.

Rothwell, R. G. (1995), Marion Dufresne Cruise 81 cruise report: Mediterranean giant piston coring transect, 17th January–9th February, 1995, Marseille, France–Limassol, Cyprus, report, 77 pp., Southampton Oceanogr. Cent., Southampton, U. K.

Sachs, J. P., and D. J. Repeta (1999), Oligotrophy and nitrogen fixation during Eastern Mediterranean sapropel events, *Science*, *286*(5449), 2485–2488, doi:10.1126/science.286.5449.2485.

Sarmiento, J. L., T. Herbert, and J. R. Toggweiler (1988), Mediterranean nutrient balance and episodes of anoxia, *Global Biogeochem. Cycles*, *2*(4), 427–444, doi:10.1029/GB002i004p00427.

Siokou-Frangou, I., U. Christaki, M. G. Mazzocchi, M. Montresor, M. Ribera d'Alcalà, D. Vaqué, and A. Zingone (2010), Plankton in the open Mediterranean Sea: A review, *Biogeosciences*, *7*(5), 1543–1586, doi:10.5194/bg-7-1543-2010.

Slomp, C. P., J. Thomson, and G. J. de Lange (2002), Enhanced regeneration of phosphorus during formation of the most recent eastern Mediterranean sapropel (S1), *Geochim. Cosmochim. Acta*, *66*(7), 1171–1184, doi:10.1016/S0016-7037(01)00848-1.

Stratford, K., and K. Haines (2002), Modeling nutrient cycling during the eastern Mediterranean transient event 1987–1995 and beyond, *Geophys. Res. Lett.*, *29*(3), 1035, doi:10.1029/2001GL013559.

Struck, U., K.-C. Emeis, M. Voß, M. D. Krom, and G. H. Rau (2001), Biological productivity during sapropel S5 formation in the Eastern Mediterranean Sea: Evidence from stable isotopes of nitrogen and carbon, *Geochim. Cosmochim. Acta*, *65*(19), 3249–3266, doi:10.1016/S0016-7037(01)00668-8.

Theocharis, A., E. Balopoulos, S. Kioroglou, H. Kontoyiannis, and A. Iona (1999), A synthesis of the circulation and hydrography of the South Aegean Sea and the Straits of the Cretan Arc (March 1994–January 1995), *Prog. Oceanogr.*, *44*(4), 469–509, doi:10.1016/S0079-6611(99)00041-5.

Thomson, J., D. Crudeli, G. J. de Lange, C. P. Slomp, E. Erba, C. Corselli, and S. E. Calvert (2004), *Florisphaera profunda* and the origin and diagenesis of carbonate phases in eastern Mediterranean sapropel units, *Paleoceanography*, *19*, PA3003, doi:10.1029/2003PA000976.

Triantaphyllou, M., et al. (2009), Late Glacial–Holocene ecostratigraphy of the south–eastern Aegean Sea, based on plankton and pollen assemblages, *Geo Mar. Lett.*, *29*(4), 249–267, doi:10.1007/s00367-009-0139-5.

Triantaphyllou, M., A. Antonarakou, M. Dimiza, and C. Anagnostou (2010), Calcareous nannofossil and planktonic foraminiferal distributional patterns during deposition of sapropels S6, S5 and S1 in the Libyan Sea (Eastern Mediterranean), *Geo Mar. Lett.*, *30*(1), 1–13, doi:10.1007/s00367-009-0145-7.

Turley, C. M., M. Bianchi, U. Christaki, P. Conan, J. R. W. Harris, S. Psarra, G. Ruddy, E. D. Stutt, A. Tselepides, and F. V. Wambeke (2000), Relationship between primary producers and bacteria in an oligotrophic sea - the Mediterranean and biogeochemical implications, *Mar. Ecol. Prog. Ser.*, *193*, 11–18, doi:10.3354/meps193011.

Ujiie, H., Y. Tanaka, and T. Ono (1991), Late Quarternary paleoceanographic record from the middle Ryukyu Trench slope, northwest Pacific, *Mar. Micropaleontol.*, *18*(1–2), 115–128, doi:10.1016/0377-8398(91)90008-T.

Van Os, B. J. H., L. J. Lourens, F. J. Hilgen, G. J. De Lange, and L. Beaufort (1994), The formation of Pliocene sapropels and carbonate cycles in the Mediterranean: Diagenesis, dilution, and productivity, *Paleoceanography*, *9*(4), 601–617, doi:10.1029/94PA00597.

Wu, P., and K. Haines (1996), Modeling the dispersal of Levantine Intermediate Water and its role in Mediterranean deep water formation, *J. Geophys. Res.*, *101*(C3), 6591–6607, doi:10.1029/95JC03555.

Wüst, G. (1961), On the vertical circulation of the Mediterranean Sea, *J. Geophys. Res.*, *66*, 3261–3271, doi:10.1029/JZ066i010p03261.

Yılmaz, A., and S. Tuğrul (1998), The effect of cold- and warm-core eddies on the distribution and stoichiometry of dissolved nutrients in the northeastern Mediterranean, *J. Mar. Syst.*, *16*(3–4), 253–268, doi:10.1016/S0924-7963(97)00022-5.

Zavatarielli, M., and G. L. Mellor (1995), A numerical study of the Mediterranean Sea Circulation, *J. Phys. Oceanogr.*, *25*(6), 1384–1414, doi:10.1175/1520-0485(1995)025<1384:ANSOTM>2.0.CO;2.

Zervakis, V., D. Georgopoulos, and P. G. Drakopoulos (2000), The role of the North Aegean in triggering the recent Eastern Mediterranean climatic changes, *J. Geophys. Res.*, *105*(C11), 26,103–26,116, doi:10.1029/2000JC900131.

Ziegler, M., E. Tuenter, and L. J. Lourens (2010), The precession phase of the boreal summer monsoon as viewed from the eastern Mediterranean (ODP Site 968), *Quat. Sci. Rev.*, *29*(11–12), 1481–1490, doi:10.1016/j.quascirev.2010.03.011.

Ziveri, P., R. C. Thunell, and D. Rio (1995), export production of coccolithophores in an upwelling region: Results from San-Pedro Basin, Southern California Borderlands, *Mar. Micropaleontol.*, *24*(3–4), 335–358, doi:10.1016/0377-8398(94)00017-H.

Ziveri, P., A. Rutten, G. J. de Lange, J. Thomson, and C. Corselli (2000), Present-day coccolith fluxes recorded in central eastern Mediterranean sediment traps and surface sediments, *Palaeogeogr. Palaeoclimatol. Palaeoecol.*, *158*(3–4), 175–195, doi:10.1016/S0031-0182(00)00049-3.

Ziveri, P., K. H. Baumann, B. Bockel, J. Bollmann, and J. R. Young (2004), Biogeography of selected Holocene coccoliths in the Atlantic Ocean, in *Coccolithophores: From Molecular Processes to Global Impact*, edited by H. R. Thierstein and J. R. Young, pp. 403–428, Springer, Berlin.